An Introduction to Seismic Interpretation

R McQuillin M Bacon W Barclay

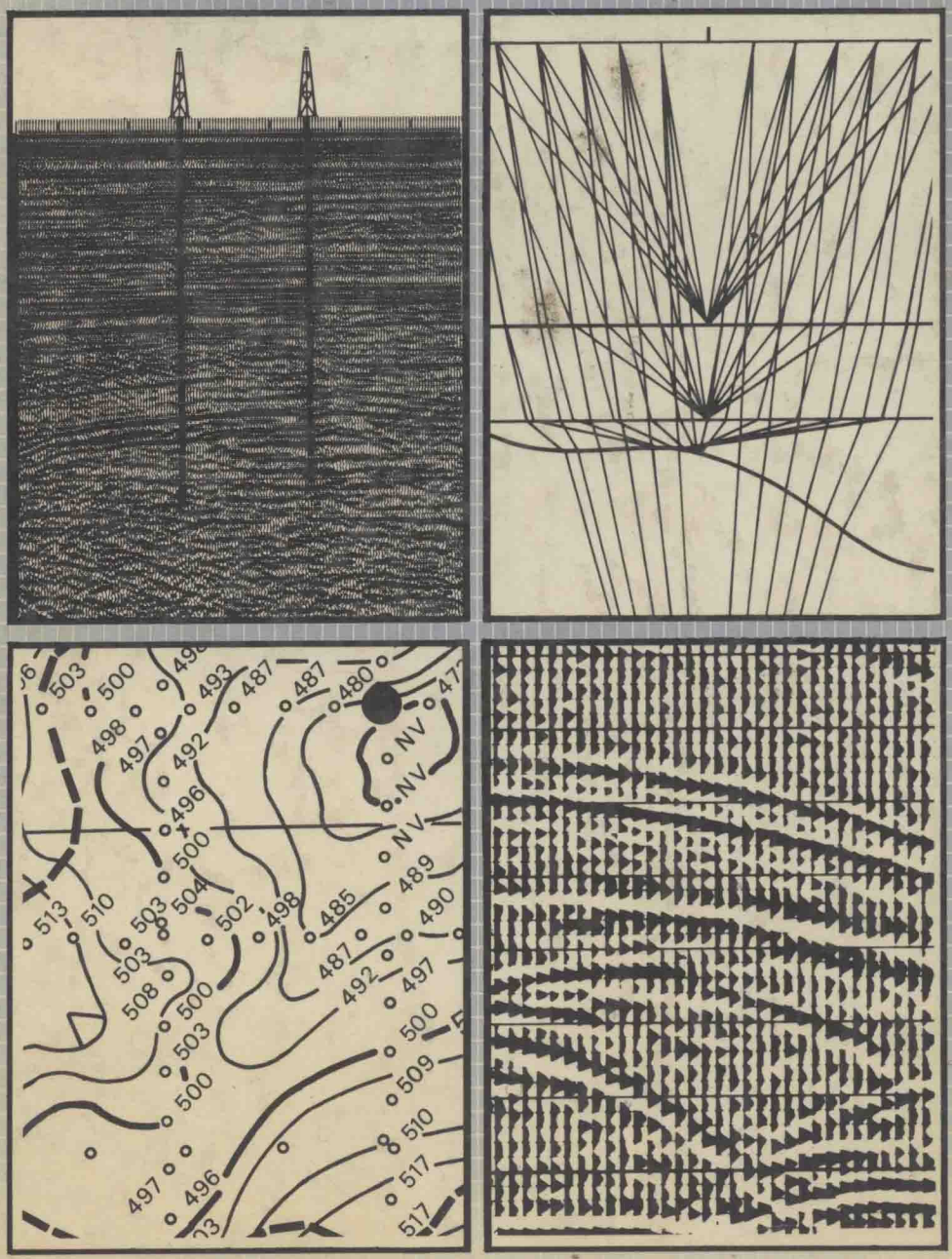

Graham & Trotman Limited

An Introduction to Seismic Interpretation

R McQuillin M Bacon W Barclay

Graham & Trotman Limited

First published in 1979 by
Graham & Trotman Limited
Bond Street House
14 Clifford Street
London W1X 1RD, United Kingdom

ISBN: 0 86010 111 8

CONTENTS

PREFACE

This book was commenced in 1976 when all three principal authors were working in Edinburgh. Chapters one to eight form the main text of the book whereas the final four chapters are case histories which aim to illustrate the application of interpretational techniques to a range of specific exploration problems.

The main text is a joint collaboration between the three authors, with primary responsibility falling to Robert McQuillin. The Moray Firth case study was prepared by M. Bacon, the Rainbow Lake and Hewett chapters by W. Barclay and we are indebted to Esso Australia for approving preparation of the Kingfish study by two of their staff, David McEvoy and Ron Steele. Robert McQuillin undertook the task of editing material for publication.

The authors wish to acknowledge their indebtedness to:
The Director of the Institute of Geological Sciences for his permission to publish a number of I.G.S. photographs and open-file records and publications for some of the illustrations; for approving the participation of McQuillin and Bacon in the publication of this book.
Enserch Canadian Exploration Limited for approval of the participation of William Barclay.
Linda Nisbet for secretarial assistance and Angela McQuillin for her work on preparing the illustrations.

Many companies have given valuable assistance by providing information on equipment, examples of various types of geophysical records and material for illustrations. The addresses of companies referred to in the text are supplied in appendix 2.

R McQuillin
Edinburgh

M Bacon
Legon

W Barclay
Calgary

March 1979

1. SEISMIC WAVES

The object of seismic reflection prospecting is to delineate subsurface geological structures using the ability of some horizons within the earth to reflect sound waves. This chapter sketches briefly the elementary theory of seismic waves, and discusses their behaviour in the real earth.

1.1 Elasticity

Seismic waves are elastic waves propagating through the earth; we therefore begin by briefly considering the basic definition of elasticity. For many materials subjected to small applied forces, Hooke's Law holds good; the deformation produced is proportional to the applied force. Consider a length of rubber being stretched by a weight (figure 1/1b). If the original length of the specimen is L and the extension produced is e, we define the strain for this type of deformation as e/L. For a given weight (ie stretching force) the extension produced will depend on the thickness of the specimen. We therefore define the stress as the force acting per unit area. Then Hooke's Law states:

$$\frac{\text{stress}}{\text{strain}} = \text{constant}$$

so in our case of longitudinal stress this becomes:

$$\frac{\text{longitudinal applied force/cross-sectional area}}{\text{change in length/original length}} = Y$$

where Y is a constant, characteristic of the material of the specimen, called Young's modulus.

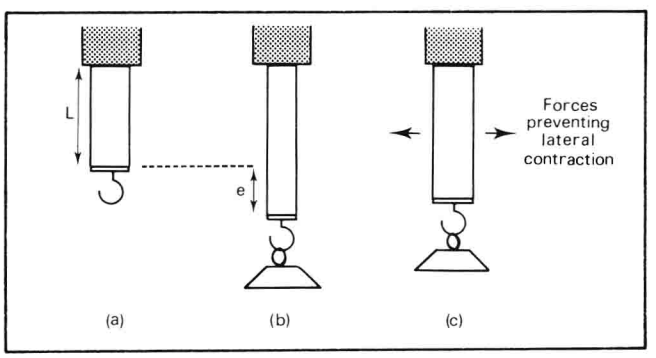

Figure 1/1: Deformation of rubber under applied force.

In the situation of figure 1/1b, when the specimen is stretched not only does its length increase but its width is decreased. We could imagine a situation similar to figure 1/1c when lateral forces are applied to prevent this decrease in width; this is similar to the situation in the solid earth, for when a given section of rock is pulled in a given direction the rocks on either side tend to prevent lateral contraction. The effect of these lateral forces is to decrease the extension under the applied load. In this situation the ratio of longitudinal applied stress to strain is still a constant, called the axial modulus Ψ. We note that the axial modulus will be greater than Young's modulus.

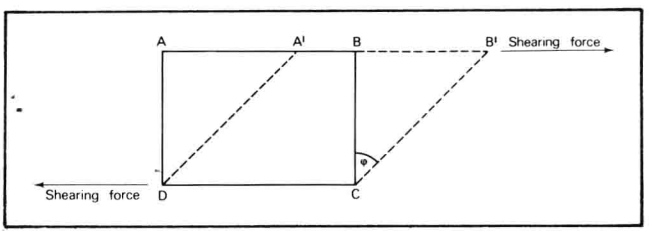

Figure 1/2: Shear deformation.

Another type of deformation is shear, which affects shape but not volume (figure 1/2). The cross-section ABCD is distorted to A'B'CD. Hooke's Law now takes the form:

$$\frac{\text{shearing force/unit area}}{\text{angular deformation } (\varphi)} = \text{constant} = \mu$$

μ is a characteristic of the material and is called the rigidity modulus.

1.2 P and S waves

Elastic waves are of two main types. In longitudinal waves, called P waves by seismologists, the direction of particle motion is parallel to the direction of wave propagation, whereas in transverse waves (S waves) these directions are perpendicular to each other. The P waves are essentially ordinary sound waves.

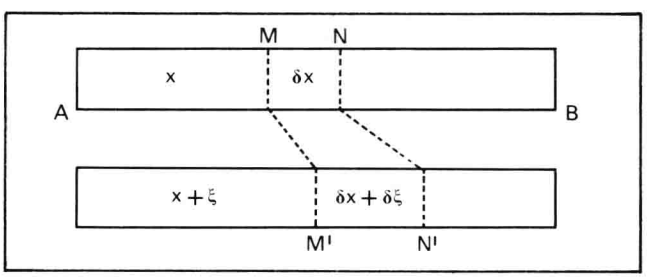

Figure 1/3 Longitudinal waves in a bar.

The example of longitudinal waves in a bar demonstrates how the equation governing these waves can be derived. Figure 1/3 shows a bar AB of cross-sectional area α, of Young's modulus Y, and of density ρ. As a longitudinal wave passes along the rod, each element of the bar vibrates parallel to the rod. The element MN is displaced to a new position $M'N'$. At M' the tension is given by Hooke's Law:

$$T_{M'} = Y \cdot \frac{\text{change in length}}{\text{original length}} = Y \cdot \frac{\delta\xi}{\delta x_{M'}}$$

Thus the force on this element is:

$$(T_{N'} - T_{M'})\,a = Ya\left(\frac{\delta\xi}{\delta x_{N'}} - \frac{\delta\xi}{\delta x_{M'}}\right) = Ya.\,\delta x.\frac{d^2\delta}{dx^2},$$

and since the mass of this element is $\alpha.\delta x.\rho$ and its acceleration is $\frac{d^2\xi}{dt^2}$

$$Ya.\delta x.\frac{d^2\xi}{dx^2} = a.\delta x.\rho\frac{d^2\xi}{dt^2},$$

$$\text{ie} \quad \frac{d^2\xi}{dx^2} = \frac{1}{c^2}\frac{d^2\xi}{dt^2\delta} \text{ where } c^2 = \frac{Y.}{\rho} \qquad (1)$$

Equation (1) is the usual equation of wave motion satisfied by any function of the form $f(x + ct)$, which represents a wave propagating with velocity c.

A similar analysis for the case of a longitudinal wave in the solid earth (a P wave) shows that it propagates with a velocity given by $\sqrt{\Psi/\rho}$ where Ψ is the axial modulus, because a lateral contraction of the volume element is prevented by the surrounding rock. It can be shown that for S waves, involving displacements perpendicular to the direction of wave propagation, the velocity is given by $\sqrt{\mu/\rho}$ where μ is the shear modulus.

In seismic reflection prospecting, only P waves are generally encountered. This is because seismic sources generate almost exclusively P waves; in marine work, the source is surrounded by water, in which case the S waves could not propagate even if they were generated. (Fluids have zero resistance to shear and therefore cannot sustain S waves; formally, if $\mu = 0$ the velocity is zero). However, S waves can be generated where P waves strike an interface at inclined incidence, and are therefore of some importance in seismic reflection work (p.95); in seismic reflection practice, the angles of incidence are normally too small for appreciable conversion to occur.

The amplitude of vibration of the particles transmitting the seismic wave may be extremely small; in the case of reflections from a depth of several kilometres, the amplitude may be only a few angstroms.

1.3 Seismic velocities in rocks and fluid media

We have seen in the last section how to calculate the seismic wave velocity in a single medium. The next step in working towards calculation of seismic velocities in the real earth is to consider a mixture of two components, each of known velocity. Immediately we are in difficulties. At frequencies of interest in reflection seismics, the wavelength of a signal may be several hundred metres, so the seismic wave will not 'see' individual grains of the mixture. A useful starting point is the time-average equation.

$$\frac{1}{c} = \frac{1-\Phi}{c_1} + \frac{\Phi}{c_2},$$

where c is the velocity of a mixture containing a fraction ϕ of material of velocity c_2 in a matrix of velocity c_1. This equation is derived from a model in which the two components of the mixture are physically separated (figure 1/4). In this case the time taken for the seismic waves to transverse a length L of mixture will be:

$$t = \frac{(1-\Phi)L}{c_1} + \frac{\Phi L}{c_2},$$

giving an average velocity c where

$$\frac{1}{c} = \frac{t}{L} = \frac{1-\Phi}{c_1} + \frac{\Phi}{c_2}.$$

It is hard to give much justification for this model, and indeed the time-average equation is of restricted application, as we shall see.

Suppose now that our model earth is still dry, but no longer solid; that is, let it contain empty pore space. A very simple physical model suggests that modest porosity will reduce seismic velocities markedly. In figure 1/5 we divide the rock into columns parallel to the direction of travel of the seismic signal; initially these are in close contact. Porosity is then introduced by moving the columns apart slightly. The average density is reduced, but so is the elasticity because the gaps between the columns contribute nothing to the stiffness of the material. The effects of these changes on the seismic velocity cancel one another out. However, the columns are now able to deform sideways, so we must use Young's modulus rather than the axial modulus in calculating the seismic velocity. Therefore there will be a drastic decrease in velocity. Recollecting that the amplitude of particle displacement in a seismic wave may be only a few angstroms, we see that fractures too small to detect optically could have a marked effect on velocity. The implication is that a very small amount of gas-filled porosity would produce a marked reduction in

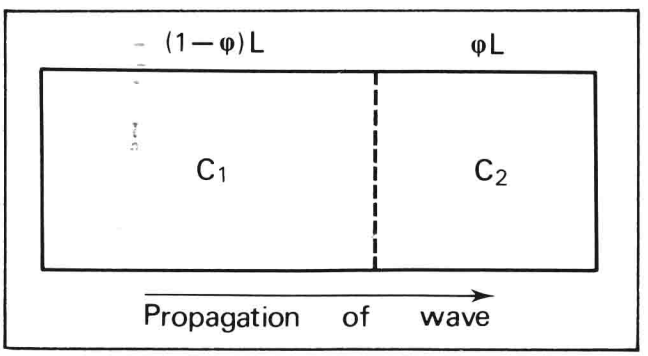

Figure 1/4: Derivation of the time average equation.

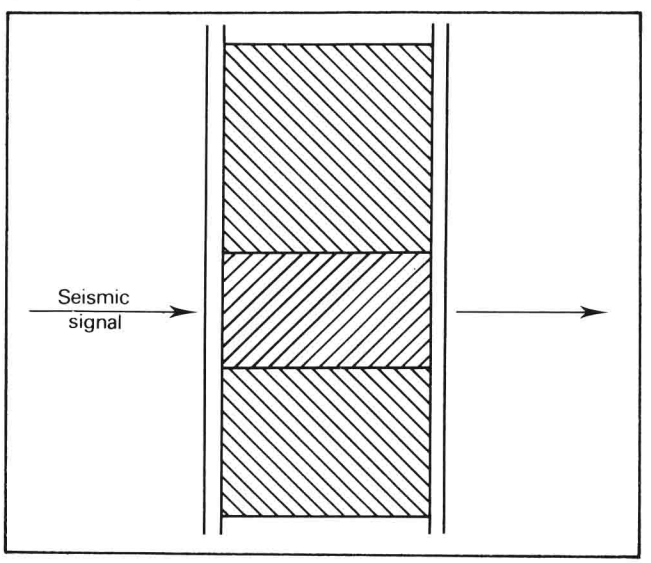

Figure 1/5: Model to illustrate the effect of porosity on velocity in a column of rock.

seismic velocity; this is of great importance for direct hydrocarbon detection (see p.119). Velocities less than that of sound in seawater are sometimes observed in gas-bearing strata.

If the pores are filled with liquid, the situation is more complicated because the liquid tends to resist the lateral deformation of the rock, and the time-average equation may apply. This is true for limestones and for sandstones whose depth of burial exceeds about 2km. At shallow levels, sandstone velocities tend to be unpredictable due to non-consolidation and variable fluid pressure gradients. Thus for a wet sandstone below 2km or a limestone we can write:

$$\frac{1}{c} = \frac{1 - \Phi}{c_1} + \frac{\Phi}{1.5}$$

where c is in km/sec, ϕ is the porosity and c_1 is the matrix velocity, say 5.7km/sec for sandstones and 6.6km/sec for limestones.

Velocities in shales are often well predicted from a relationship between velocity (c) and depth burial (Z) of the type

$$Z = A + B \cdot \ln c$$

where A and B are constants for a given area.

Some typical observed velocities are shown in table 1/1. In general, igneous rocks have higher velocities than sedimentary rocks.

Table 1/1 : Typical ranges of P wave velocities in rocks. (after Grant and West, 1965).

Material	*Velocity, km/s*
Salt and anhydrite	4.9 – 6.9
Granites and metamorphics	4.0 – 5.8
Limestone and dolomite	2.7 – 5.2
Sandstone and shale	0.8 – 3.4

1.4 Densities of rocks and fluid media

In the next section we shall need some knowledge of rock densities. For this case, the theoretical background to the treatment of mixtures and porous material is much more soundly based than for velocities. As in the case of the derivation of the time-average equation, the model requires the separation of the constituents into two partitions of the volume; the validity of this procedure is not in doubt for densities. We then derive that the average density ρ is given by

$$\rho = (1 - \Phi)\rho_1 + \Phi\rho_2$$

where a fraction ϕ has the density ρ_2 and the matrix has density ρ_1. This can obviously be extended to any number of constituents.

For shales, a very significant increase of density with depth occurs; this compaction is largely due to rearrangement of clay particles and is not recovered if the pressure is subsequently reduced by removal of the overburden. As compaction becomes complete, the density tends to about 2.3 g/cc.

Table 1/2: Typical ranges of Rock Densities.

Material	*Density, gm/cc*
Igneous rocks	2.5 – 2.9
Limestone	2.3 – 2.8
Shale	2.0 – 2.7
Sandstone	2.1 – 2.6
Salt	1.9 – 2.1

Some typical observed densities are shown in table 1/2.

1.5 Reflection of seismic waves

If a plane seismic wave strikes a plane interface between two different materials, it will be partially reflected and partially transmitted. For the case of normal incidence we can calculate the reflection coefficient (ie the ratio of the amplitudes of the reflected and incident waves) as follows. If we consider a sinusoidal wave of frequency υ incident at the interface (figure 1/6), it will be described by the equation:

$$\xi = \xi_I \exp 2\pi i\upsilon(t - x/c_1)$$

where ξ is the displacement at time t, the distance x being measured perpendicular to the interface.

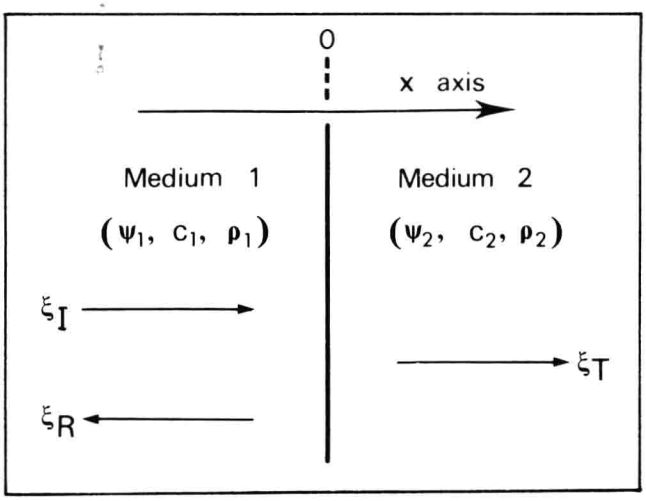

Figure 1/6: Calculation of reflection coefficient at normal incidence. ξ_I, ξ_T and ξ_R are the displacements of incident, transmitted and reflected waves. ψ_1, c_1 and ρ_1 are the axial modules, velocity and density of medium 1; ψ_2, c_2, ρ_2 those of medium 2.

The reflected and transmitted waves will be:

$$\xi = \xi_R \exp 2\pi i\upsilon(t + x/c_1)$$

and

$$\xi = \xi_T \exp 2\pi i\upsilon(t - x/c_2) \text{ respectively.}$$

At the interface both displacement and pressure must be continuous. Therefore, if the interface is at $x = 0$, the displacement condition gives

$$\xi_I + \xi_R = \xi_T \qquad (2)$$

and, recollecting that the pressure is given by $\frac{\Psi.S\xi}{Sx}$ we see that the pressure condition gives

$$-\frac{\psi_1.\xi_I}{c_1} + \frac{\psi_1.\xi_R}{c_1} = -\frac{\psi_2.\xi_T}{c_2} \qquad (3)$$

Combining (2) and (3) gives:

$$\frac{\xi_R}{\xi_I} = \frac{\psi_1/c_1 - \psi_2/c_2}{\psi_2/c_2 + \psi_1/c_1}.$$

But $c = \sqrt{\psi/\rho}$, so $\psi/c = \rho c$.

Therefore $$\frac{\xi_R}{\xi_I} = \frac{\rho_1 c_1 - \rho_2 c_2}{\rho_1 c_1 + \rho_2 c_2}. \qquad (4)$$

This is the required reflection coefficient. It is useful to define the acoustic impedance, r, by

$$r = \rho c.$$

A reflected wave will be observed whenever there is a change of acoustic impedance at an interface. The reflection coefficient for pressure amplitudes will be given by:

$$\frac{P_R}{P_I} = \frac{r_2 - r_1}{r_2 + r_1}.$$

where P_I is the pressure amplitude of the incident wave and P_R that of the reflected wave.

There will thus be a phase reversal (negative coefficient) if the incident ray is in the higher impedance material.

Some typical reflection coefficients at normal incidence are as follows:

Sea floor 1/3
Sea surface − 1 (wave incident from below).
Normal strong reflector 1/5

At inclined incidence, derivation of a general formula is difficult because partial conversion into S waves can occur. The reflection coefficient increases as the angle of incidence increases, becoming large in the vicinity of the critical angle, arcsin c_1/c_2. In seismic reflection practice, data is obtained only at near-normal incidence. Data at inclined incidence would be useful where there is no difference of acoustic impedance across an interface because c and ρ change in opposite directions. Equation (4) shows that there will be no reflection at normal incidence, but a reflection would be expected at inclined incidence. This lack of acoustic impedance contrast, despite velocity changes, is sometimes observed at salt horizons.

That part of the energy not reflected at the interface is transmitted into the second medium, undergoing refraction at the interface; the angle of refraction is related to the angle of incidence by Snell's Law, $\sin r/\sin i = c_2/c_1$ where c_2 is the velocity on the refracted ray side and c_1 that on the incident ray side, i and r being the angles of incidence and refraction.

1.6 Absorption

Energy is lost by the seismic wave during its transit through the earth. Generally, there is a constant fractional energy loss per cycle of the seismic wave. Some values are as follows:

	Energy loss, dB/wavelength
Weathered rock, gas sands	3
Normal rock	0.5
Lowest observed	0.1

Since there is a constant fractional loss per wavelength, higher frequencies are attenuated more than lower frequencies for a particular path length. The way in which the earth behaves as a low-pass filter can be illustrated by an example. Suppose we have a reflector at a depth of 2 seconds (two-way travel time). In normal rock, the energy of the reflected signal is affected by absorption as shown in table 1/3. There is clearly a very significant loss of high-frequency energy. Even if our seismic input signal had a sharp spike wave form, so that all frequencies were equally represented, it would become a low frequency (say several tens of Hz) signal after traversing a path through the earth typical of reflection prospecting.

Table 1/3: Acoustic loss in 2s path length due to 0.5dB absorption per wavelength.

Frequency Hz	*No of wavelengths in path*	*Loss dB*
10	20	10
20	40	20
40	80	40
80	160	80

1.7 Diffraction and interference

Consider a point reflector, which reflects seismic energy back along its incoming path whatever the angle of incidence (figure 1/7). The travel time will be:

$$2(X^2 + Z_0{}^2)^{1/2}/c.$$

Therefore, if the reflection time is incorrectly assumed to come from a point vertically below the source, the point reflector will produce an apparent event at D, where AD = AB. The locus of such points is given by:

$$z = \frac{2(x^2 + z_o{}^2)^{\frac{1}{2}}}{c}$$

ie $$c^2z^2 = 4(x^2 + z_o{}^2)$$

which is a hyperbola whose apex is situated at the point reflector. An actual example is shown in figure 1/8.

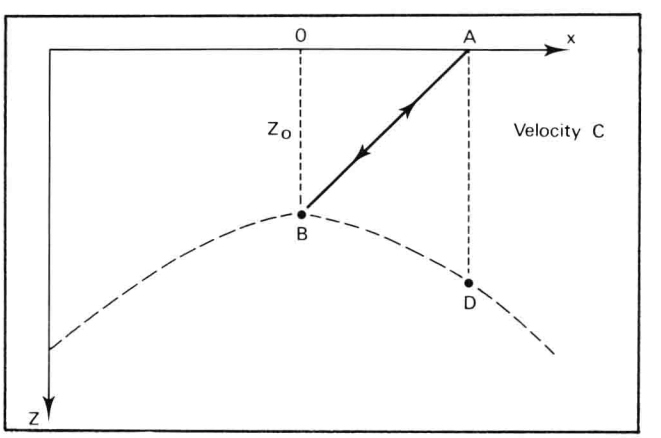

Figure 1/7: Apparent seismic event (dashed line) associated with reflection from point B.

Detailed theory of the seismic wave shows that where a reflector is suddenly terminated (eg by a fault), the end of the reflector behaves like a point source (figure 1/9). In practice, only the section BD of the hyperbola is observed. Such hyperbolic events at faults are common on seismic records (figure 1/10). This is an example of diffraction; the wave interacts with obstacles in ways different from those predicted by simple ray theory.

Another effect stemming from the wave nature of the seismic disturbance is interference. When reflections are obtained from two closely-spaced horizons, the reflected pulses overlap and it may not be possible to separate the two horizons on the seismic record. Since the wavelength of a typical seismic signal will be several hundred metres, this situation is very common and is often found in structures of hydrocarbon significance, such as wedge-outs and fluid contacts. Often such composite events can be identified by careful study of the wave-form.

1.8 Elementary propagation theory

An alternative approach to the description of how seismic waves are propagated through a medium is based on the concepts of geometrical optics, and although this topic is covered in many standard physics text books, it is useful to consider here how these principles help in the understanding of and interpretation of seismic travel times. The propagation of seismic waves through a medium causes a displacement of the individual particles within it. If we consider sinusoidal oscillations, as described in the one-dimensional case by the relation $\xi = \sin(x + ct)$, where ξ is the particle displacement and c is the seismic velocity we see that particles at different distances from the source (differing x values) are at different stages in their oscillations at any time t; that is, they have different phases. One of the ways in which the propagation of a wave may be followed is by joining together the points where the particles have a particluar phase to form a wavefront. For example, if we have a point source in a uniform medium the wavefronts will be spheres centred on the source; or, in the one-dimensional case, the wavefronts will be planes perpendicular to the x axis. A wavefront of given phase will advance with velocity c; thus in the one-dimensional case a wavefront situated at $x = x_1$ at time $t = t_1$ will at time $t = t_2$ be situated at x_2 such that:

i.e.

$$x_1 + ct_1 = x_2 + ct_2$$
$$x_2 - x_1 = c(t_1 - t_2).$$

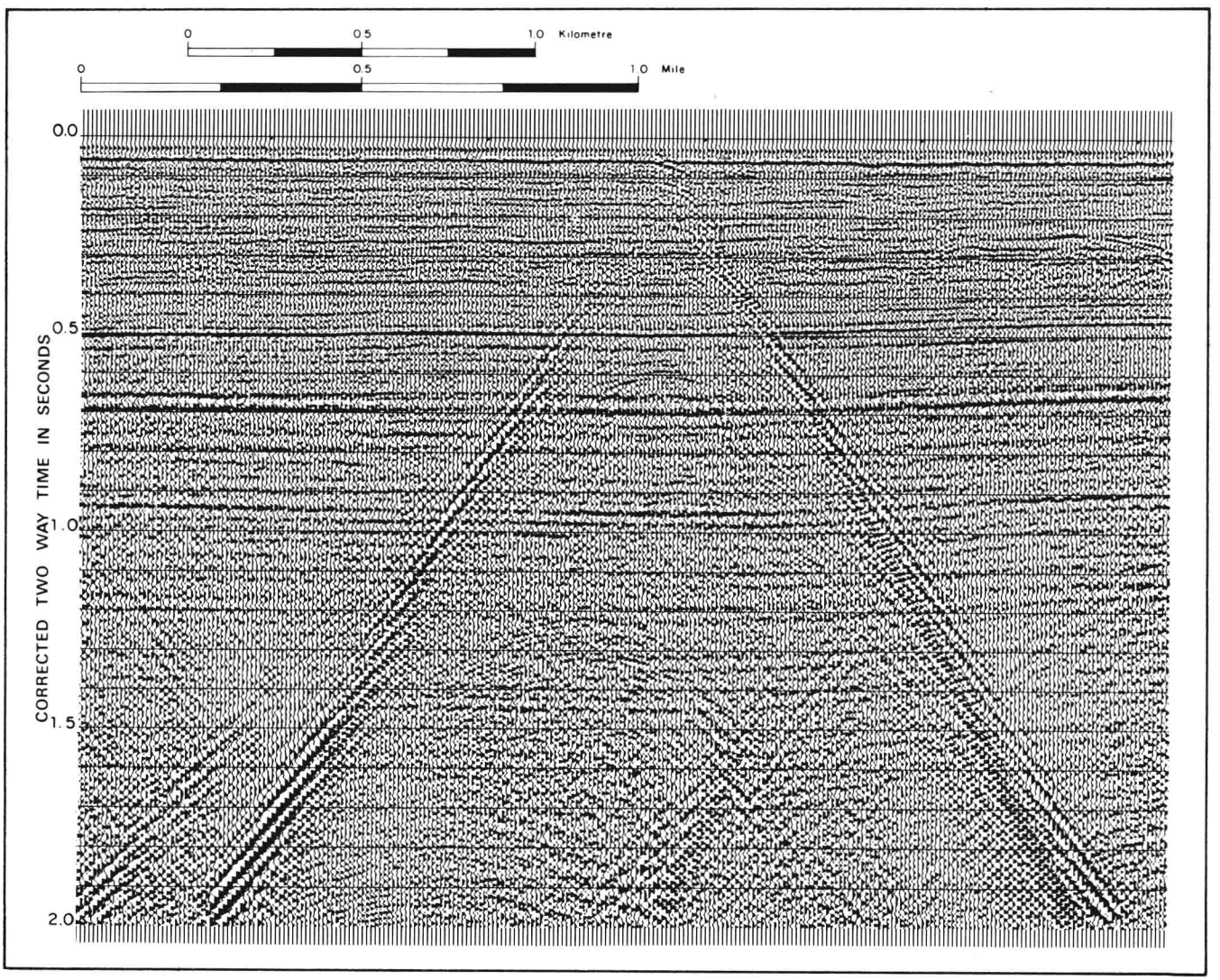

Figure 1/8: Hyperbolic event from a single-point reflector.
(Courtesy: IGS, S&A record).

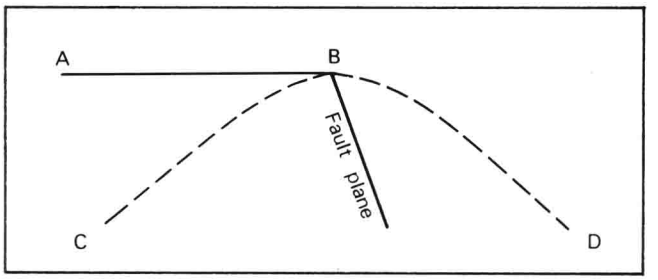

Figure 1/9: Theoretical diffraction pattern from a fault.

The wavefront is propagating in the negative x direction at a velocity c.

The mechanism by which a disturbance is propagated is that each vibrating particle exerts a force on its neighbour, causing it to vibrate. This suggests a way in which, given its initial position, the successive positions of a wavefront can be constructed: we suppose that each vibrating particle on the wavefront behaves as a point source of secondary wavelets. This is called *Huygen's Principle*. The subsequent disturbance is found by combining all these secondary wavelets; in order to explain the observed propagation it is necessary to suppose that the secondary wavelets produce an appreciable effect in the forward direction only.

A different method of depicting the propagation of the seismic disturbance is to follow the paths along which energy travels. These paths are called rays. In isotropic media the rays are perpendicular to the wavefronts in general. It is often easier to think of wave propagation in terms of rays; see for example the complex reflection pattern produced by a sharply concave reflector as illustrated in figure 3/26. The laws governing ray behaviour are simple, but ray theory is far from adequate to explain all observed propagation effects.

As described in section 1.5, when a plane seismic wave strikes a plane interface between two different materials, it will be partly reflected and partly transmitted. The geometry of this situation is illustrated in figure 1/11. As each element of the wavefront AB reaches the surface A_1B_2, it is a source of secondary wavelets.

In the reflection case, A_1 acts as a source when B is at B_1, so that by the time B gets to B_2 the secondary wavelet from A_1 has expanded to a radius A_1A_2 which also equals B_1B_2. By treating all parts of the wavefront in this way one can construct A_2B_2 as the reflected wavefront. The ray paths have the simple geometry that they are in the same

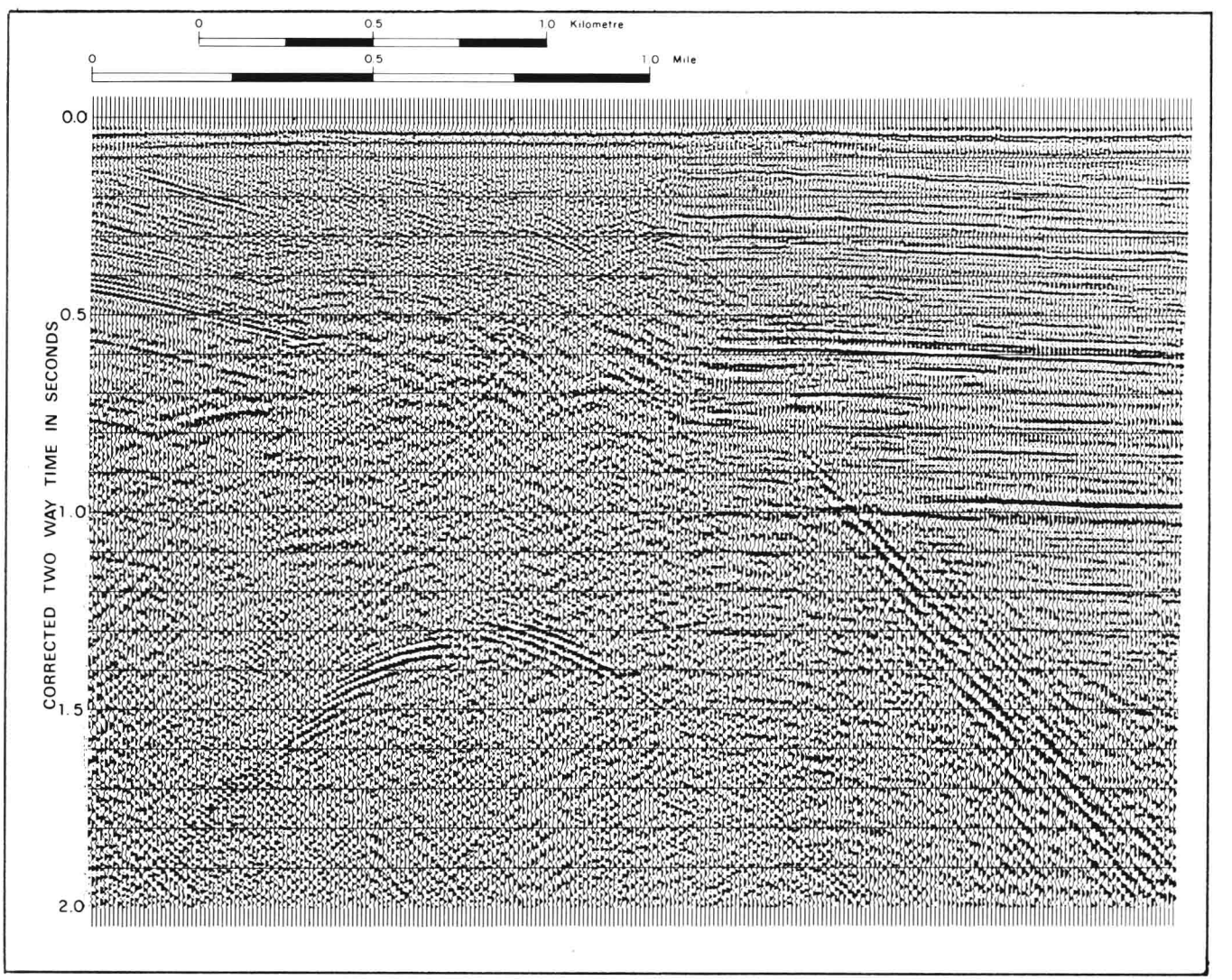

Figure 1/10: Hyperbolic diffraction patterns caused by faulting.
(Courtesy: IGS, S&A record).

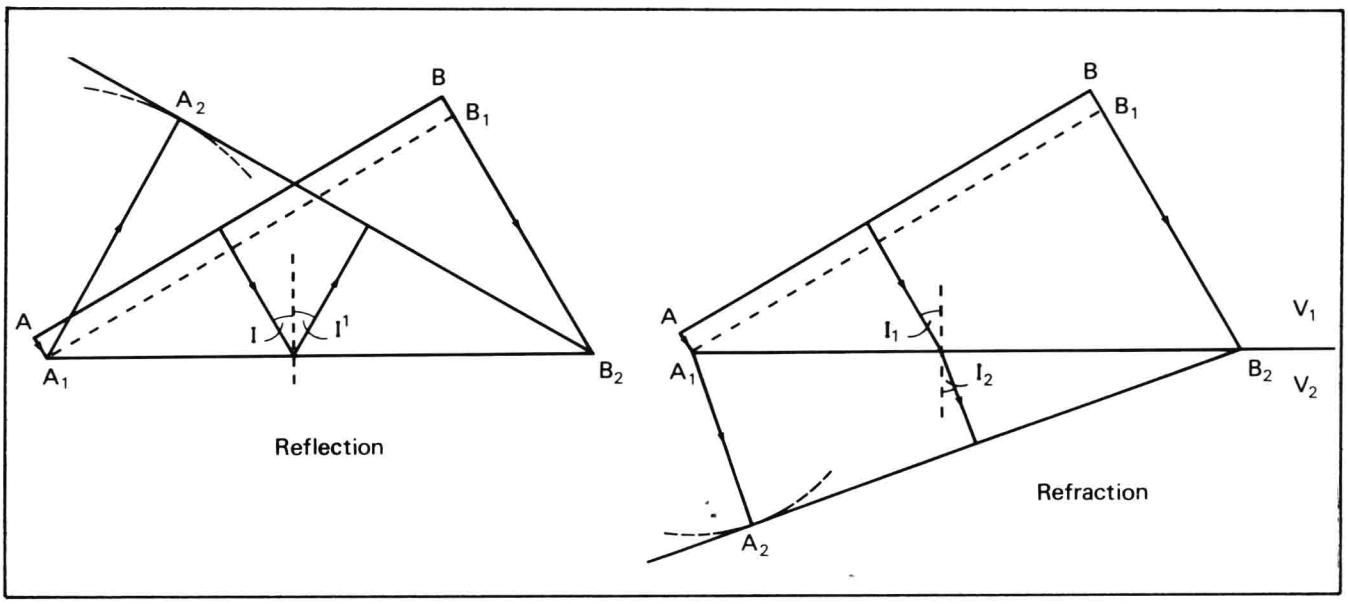

Figure 1/11: Reflection and refraction of a plane wave AB at plane interface A_1B_2.

plane as, and are equally inclined tot he normal to the reflector at the point of incidence, i.e. I = I'

In the case of the transmitted wave, we see that while the disturbance travels from B_1 to B_2, the secondary wavelet from A_1 expands to $A_1A_2 = B_1B_2,(V_2/V_1)$; in the illustration V_1 V_2 thus the distance A_1A_2 is less than B_1B_2.From the above it can be deduced that the transmitted wavefront is normal to a ray whose direction is given by:

$$\frac{\sin I_1}{\sin I_2} = \frac{V_1}{V_2}$$

The wavefront is said to have been refracted at the interface, and as before, the two wavefront normals and the normal to the refracting surface lie in the same plane. This description of the refracted wave is generally known as *Snell's Law* as noted in section 1.5.

In more complicated cases the behaviour of rays can be predicted from *Fermat's Principle* which states that the ray path along which a disturbance travels from one point to another will be that taking the least time.

1.9 Summary

1. Seismic prospecting utilises reflection of sound waves to delineate horizons within the earth.
2. A reflection occurs wherever there is a change in **acoustic impedance** (defined as the product of seismic velocity and density). The greater the impedance contrast, the stronger the reflection. Such impedance changes normally correspond to lithological variations.
3. Absorption causes the earth to act as a low-pass filter, making deep reflections rich in low frequencies compared to the input signal.
4. Hyperbolic diffraction patterns on the seismic section are generated by point reflectors and by sharp geological discontinuities such as faults and steeply inclined flanks of monoclines, synclines and anticlines.

References and suggested reading

B.S. Evenden, D.R. Stone and N.A. Anstey, *Seismic prospecting instruments.* (Gebruder Borntraeger, Berlin)

Vol. 1: *Signal characteristics and instrument specifications* by N.A. Anstey (1970).

Vol. 2: *Instrument performance and testing* by B.S. Evenden and D.R. Stone (1971).

These volumes give a full account of seismic instrumentation design and performance.

A.A. Fitch, *Seismic reflection interpretation* (Gebruder Borntraeger, Berlin, 1976). A book on seismic interpretation written at three levels: an introductory level, a professional level and a research level.

F.S. Grant and G.F. West. *Interpretation theory in applied geophysics* (McGraw-Hill Book Company, New York, 1965). A mathematical text on interpretation methods used in applied geophysics.

Seismograph Service Corporation, *The Robinson-Treitel Reader* (SSC, Tulsa, Oklahoma, 1973) A collection of papers on digital data processing compiled by SSC as a service to industry.

R.E. Sheriff, *Encyclopaedic dictionary of exploration geophysics* (Society of Exploration Geophysicists, USA, 1973). A well illustrated encyclopaedia covering the whole field of exploration geophysics.

2. DATA ACQUISITION

In this chapter we consider the application of seismic theory, as described in chapter 1, to the design of equipment for generating seismic pulses, and detecting and recording the earth's response to the passage of seismic waves through it. The aim here is not to treat the subject of data acquisition at the level which would be required in a text-book written for geophysicists principally concerned with field techniques, but to present enough background information on this subject to satisfy the needs of the seismic interpreter who may have little opportunity to participate in field surveys, or at best gain experience of only a limited range of the methods currently in use. Exploration seismology is a remote-sensing technique in which the aim is to record as detailed a picture as possible of subsurface geology. The product of a seismic investigation is a geological model which can be described as the sum of a finite series of layers of varying thickness, physical properties (density and seismic velocity) and structural attitude. Interpretation of this model is in terms of geological structure, lithological variation, stratigraphy and, in oil exploration, hydrocarbon prospectivity.

Seismic data is acquired using a system consisting of three main components: an input source, an array of detectors and a recording instrument. The input source is designed to generate a pulse of sound which meets, as near as possible, certain predefined requirements of total energy, duration, frequency content, maximum amplitude and phase. Reflected and refracted seismic pulses (the output from the earth) are detected by an array of geophones or a hydrophone array, then recorded by a recording instrument, and in both cases these output signals will be modified by the response characteristics of that part of the system. Each seismic record is thus a time record of the output signals which are generated at interfaces in a series of stratigraphic layers because of the changes in acoustic impedance which occur at such boundaries, modified firstly by transmission decay and noise interference in the earth and then by detector and recorder response characteristics. This can be summarised as follows:

*Recorded signal = Source pulse * [Reflectivity * (Earth filter + Noise)] * Detector response * Recording instrument response,*

where * represents convolution (see p.188)

Assuming that we know the signal characteristics of the seismic pulse and the response characteristics of detector and recording instrument, then we can separate that part of the function contained in square brackets, and this is the earth's impulse response. The earth's reflectivity is what we wish to measure. The earth's filter is a variable function of absorption and attentuation which can be compensated for in data processing. Noise cannot be so adequately treated by data processing and, as far as possible, must be measured and compensated for during data acquisition. This is mainly achieved by layout design, on land by proper design of geophone spreads and arrays and at sea by use of well designed hydrophone arrays. Display of the recorded signal will not, in most situations, give an easily interpretable picture of geological structure. This record needs further processing to achieve such clarification, and these processing techniques are the subject of the following chapter.

2.1 Layout design

In designing layout systems, the emphasis is placed on eliminating unwanted signals or 'noise' of both the random and coherent variety. Use of multiple sources, multiple detectors per trace, and the summing of common reflection point traces (see figures 2/1 and 3/6) brings about a distinct improvement in signal to noise ratio in the case of random noise. For spatially random noise, the improvement is proportional to $\sqrt{n}$ where n is the number of detecting elements in the acquisition system, the signals from which are added together to provide the final record. For example, the summing of eight separate seismic signals (eight shots at same shot-point location), detected by geophone spreads of twenty geophones per trace then subject, during processing, to twenty-four fold stacking, will provide an improvement ratio of $\sqrt{8 \times 20 \times 24} = 62$ or 36dB. This may be compared with a single shot record, single-fold processed with, as before 20 geophones per spread, in which case the improvement ratio is $\sqrt{20} = 4.5$ or 13dB. The former acquisition method shows a relative improvement of 23dB over the latter in signal to noise ratio enhancement.

Figure 2/1 shows a typical marine multi-channel acquisition system and illustrates how data are acquired in a way which allows stacking during processing. Although this illustration shows only a marine system, acquisition of land data is based on identical principles. At sea, a survey ship tows a hydrophone streamer made up of a number of sections, numbered one to forty-eight in the figure. Modern streamers are fitted with 24, 48 or 96 such sections and each section consists of a group of hydrophones which are pressure sensitive sound detectors (see p.26) Signals received by the hydrophones in each section are summed so that each section is considered to be an independent single detector. In figure 2/1 the reflections from a single horizon are schematically portrayed as received in the first eight sections of the 48-section streamer. Let us assume that the distance between sections is 50m and that the ship is travelling at 8km/h (approximately 4kts). If the first shot S_1 occurs at time t_1, a reflection from depth point no.1 is received in section no.1 of the streamer and thence

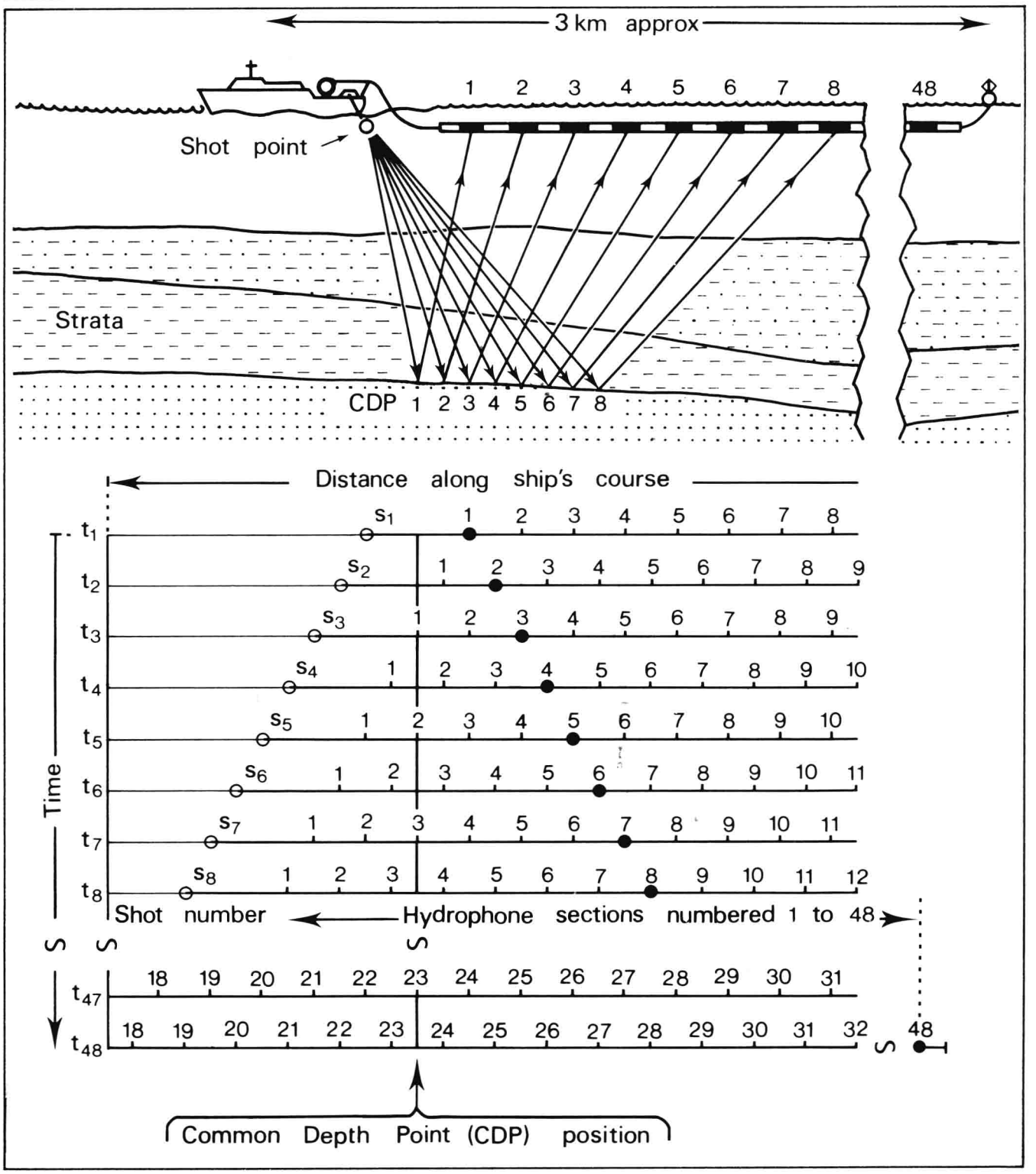

Figure 2/1: Schematic diagram showing the use of multi-channel hydrophone streamers to acquire data which can be common depth point (CDP) stacked.

recorded in channel no.1 of the seismic recording system onboard ship. The common depth point (CDP) position is located mid-way between the locations of S_1 and section no.1; in the lower half of the diagram at t_1 the section no.1 location highlighted as a large dot. The next shot S_2 is timed so that the ship has progressed to a position such that the location of the midway point between source and section no.2 of the streamer is the same CDP location as for S_1. This occurs at t_2, see lower half of diagram, and it can be seen that the distance between S_1 and S_2 is half the distance between sections, that is 25m. The interval between shots ($t_2 - t_1$) should be set therefore at 11.25s.

At t_2, the signals recorded on channel no.2 of the recording system are therefore those associated with CDP no.1. Shots S_3 to S_{48} follow at the same interval and successive records are obtained on ship from CDP 1, until data from shot S_{48} is recorded on channel no.48 of the recording system. It should be noted that as the ship progresses along course, the seismic signal reflected from CDP 1 will have travelled an ever increasing distance between shot-point and receiving streamer section. The change in geometry is corrected for during processing, and it is possible to add together (stack) all 48 records pertaining to CDP 1. Obviously the same is true for the locations CDP 2, 3 etc. CDP stacking is valuable not only as a means of increasing signal to noise ratio but also, during processing (see chapter 3), of allowing differentation between primary reflections from geological structure, and multiple reflections in sea and rock layers. Multiple reflections can then be suppressed to improve the quality of the final seismic section display. In land surveys, shot-point locations are surveyed at fixed intervals and groups of geophones are pegged into the ground with a group interval which is equivalent to the section interval of the marine streamer. Obviously, surveys on land cannot be conducted with the speed of a marine survey, and timing of shots is irrelevant to a static layout, nevertheless, the geometrical principles are identical.

Coherent noise, of the types illustrated in figure 2/2, can be reduced in two ways depending on whether it is a direct near horizontal wave originating near ground level, in the sea or near seabed, or is a reflected near vertical travelling wave. In general, lowest velocity direct waves arrive latest, a factor which can be utilised in design criteria for detector arrays. With reflected noise waves, lowest velocity waves arrive earliest and this can be utilised in the design of optimum trace spacing for attenuation stacking.

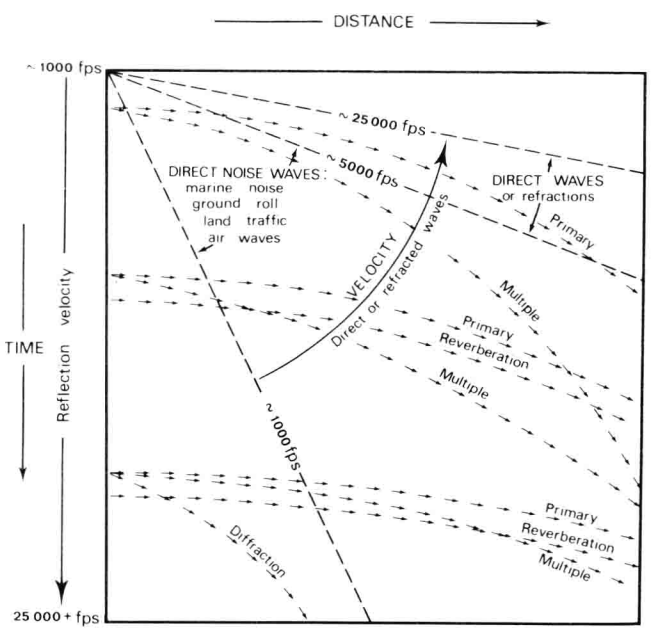

Figure 2/2: Coherent seismic noise types. For primary and multiple reflections the average velocities increase and the normal moveouts decrease with time (after S.D. Brasel in unpublished report, *Design of seismic field techniques.* Atlantic Richfield, 1971)'.

Multiple, or secondary, reflections (as opposed to the primary reflections on which data are being sought) can be attenuated or even effectively eliminated by common reflection point (or common depth point, CDP) stacking. The principle is to design the trace spacing such that the secondary reflections have the appropriate residual normal moveout to be stacked out of phase and consequently much reduced in amplitude, while the primary reflections are stacked in phase by application of the correct normal moveout velocity (see chapter 3). The formulae to be utilised for the simplest cases (see figure 2/3) are as follows:

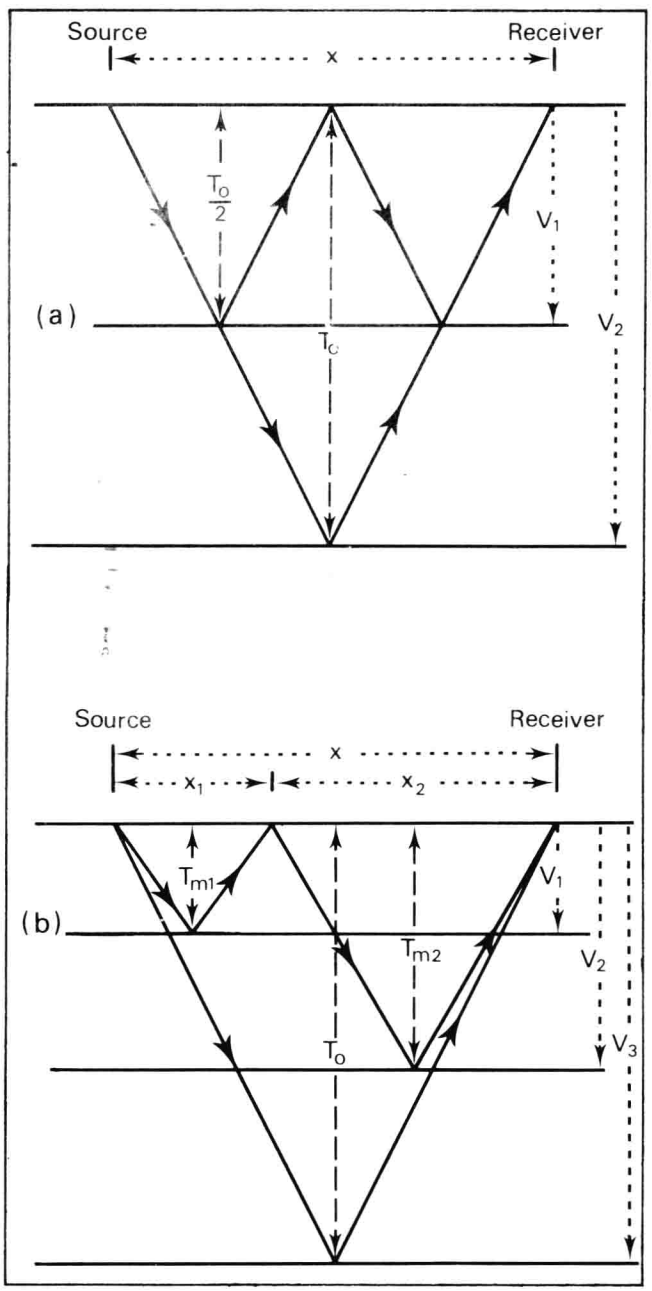

Figure 2/3: Ray path multiple reflection geometry (not adjusted for refraction according to Snell's Law).
a) First order or simple multiple.
b) Second order or peg leg multiple, that is, $T_0 = T_{m_1} + T_{m_2}$. Such multiples are common in marine survey data due to repeated reflections between seabed and sea surface.

i. The residual moveout first order (symmetrical) surface multiple equation (see figure 2/3a for definition of symbols),

$$\Delta t = \Delta T_{multiple} - \Delta T_{primary}$$
$$= 2\left(\sqrt{\frac{T_0^2}{4} + \frac{x^2}{4V_1^2}} - \frac{T_0}{2}\right) - \left(\sqrt{T_0^2 + \frac{x^2}{V_2^2}} - T_0\right)$$
$$= \sqrt{T_0^2 + \frac{x^2}{V_1^2}} - \sqrt{T_0^2 + \frac{x^2}{V_2^2}}$$

ii. The residual moveout second order (asymmetrical) or peg-leg multiple equation (see figure 2/3b for definition of symbols,)

$$\Delta t = \Delta T_{M1} + T_{M2} - \Delta T_{primary}$$
$$= \sqrt{T_{M1}^2 + \frac{x_1^2}{V_2^2}} - T_{M1} + \sqrt{T_{M2}^2 + \frac{x_2^2}{V_2^2}} - T_{M2}$$
$$- \sqrt{T_0^2 + \frac{x^2}{V_3^2}} + T_0$$
$$= \sqrt{T_{M1}^2 + \frac{x_1^2}{V_1^2}} + \sqrt{(T_0 - T_{M1})^2 + \left(\frac{x - x_1}{V_2^2}\right)^2}$$
$$\sqrt{T_0^2 + \frac{x^2}{V_3^2}}$$

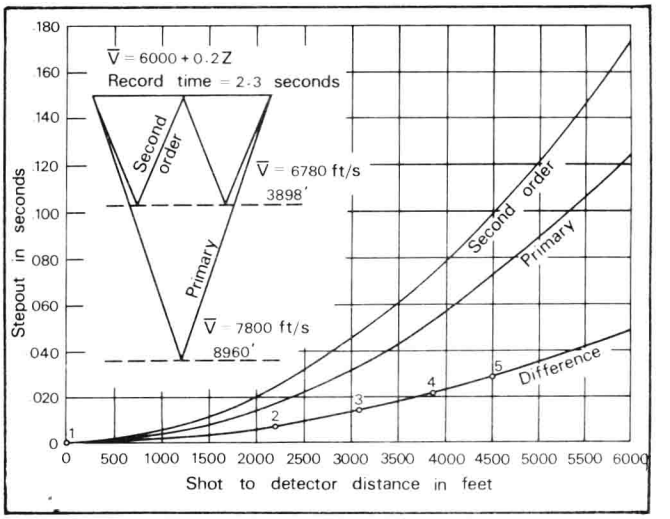

Figure 2/4: Normal moveout differentials between time-coincident primary and multiple reflections plotted against length of spread. Detector spacing across the spread could be designed to stack the second order signals (by current convention; the first order multiples) out of phase after applying normal moveout corrections to the primary signals..

For optimum attenuation, the trace distances are chosen such that the Δt differences are approximately equal to the multiple period divided by (fold of stack-1). Figure 2/4 is adapted from the original paper on stacking by Mayne* demonstrating the principle. In practice, unless expanded spreads are shot (see figure 2/5) knowledge of the type of multiple to be suppressed, and of their velocities, is usually wanting, and non-uniform trace spacing is impracticable, so the design adopted is invariably a compromise offering limited attenuation. However, it is important to be aware of the factors which control attenuation of multiples, in particular if an area is to be resurveyed with the aim of acquiring improved data in a situation where multiples are known to pose interpretation problems. Figure 2/6 is an illustration of a single-fold as against multi-fold comparison; the distinct multiple suppression and improvement in the signal to noise ratio of the primary reflections is apparent.

* W. Harry Mayne, 'Common reflection point horizontal data stacking techniques'. *Geophysics*, vol. 27, (1962) pp.927–938.

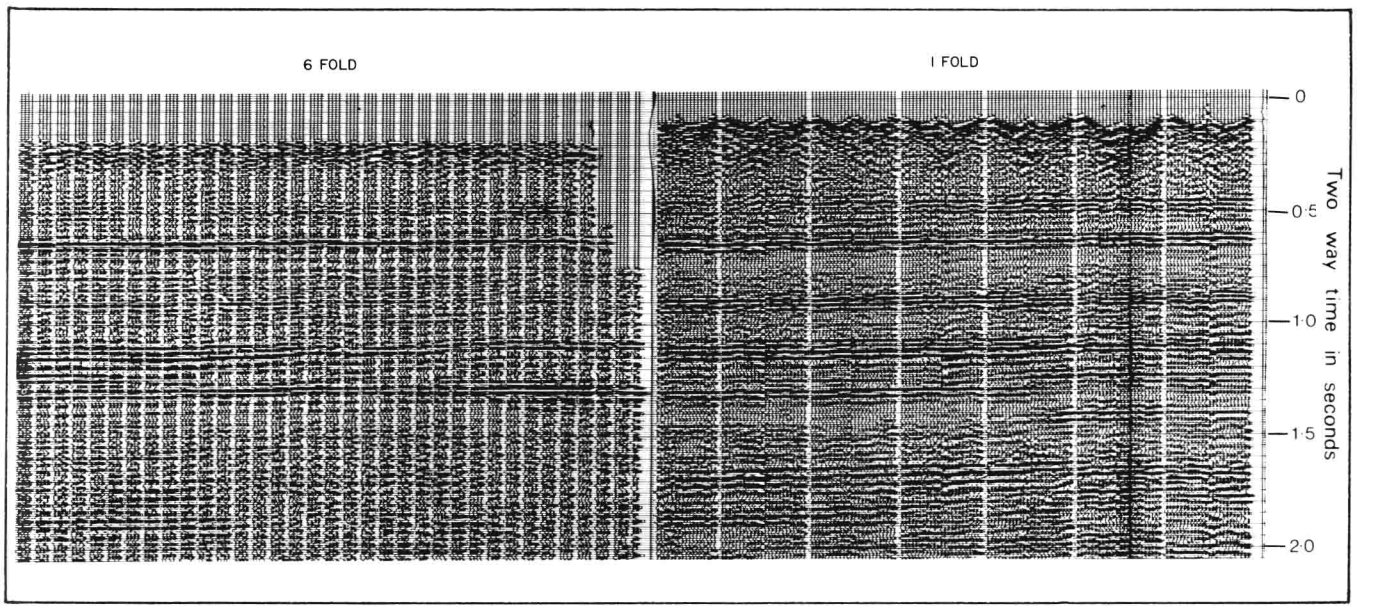

Figure 2/6: Single fold and multifold seismic section comparison. On the single fold section pronounced multiples interfere with reflections from a target horizon at between 1.05 and 1.15s two-way time.
(*Courtesy: Mobil Oil Canada Ltd*).